Dynamic Mechanical and Morphological Behavior of Blends of Polystyrene and Poly[acrylonitrile-*g*-(ethylene-*co*-propylene-*co*-diene)-*g*-styrene] Prepared by *in Situ* Polymerization of Styrene

Emerson Lourenço, Maria do Carmo Gonçalves, Maria Isabel Felisberti

Instituto de Química, Universidade Estadual de Campinas, PO Box 6154, Campinas, 13083-971, Brazil

Received 12 February 2008; accepted 18 February 2009
DOI 10.1002/app.30265
Published online 28 April 2009 in Wiley InterScience (www.interscience.wiley.com).

ABSTRACT: PS/AES blends were prepared by *in situ* polymerization of styrene in the presence of AES elastomer, a grafting copolymer of poly(styrene-*co*-acrylonitrile) – SAN and poly(ethylene-*co*-propylene-*co*-diene)–EPDM chains. These blends are immiscible and present complex phase behavior. Selective extraction of the blends' components showed that some fraction of the material is crosslinked and a grafting of PS onto AES is possible. The morphology of the noninjected blends consists of spherical PS domains covered by a thin layer of AES. After injection molding, the blends show morphology of disperse elastomeric phase morphology in a rigid matrix. Two factors could contribute to the change of morphology: (1) the stationary polymerization conditions did not allow the mixture to reach the equilibrium morphology; (2) the grafting degree between PS and AES was not high enough to ensure the morphological stability against changes during processing in the melting state. The drastic change of EPDM morphology from continuous to disperse phase has as consequence a decrease in the intensity of the loss modulus peaks corresponding to the EPDM glass transition. However, the storage modulus at temperatures between the glass transition of EPDM and PS/SAN phases does not change significantly. This effect was attributed to the presence of the SAN rigid chains in the AES. © 2009 Wiley Periodicals, Inc. Journal of Applied Polymer Science 113: 2638–2648, 2009

Key words: polystyrene; AES; blends; morphology; dynamic mechanical properties

INTRODUCTION

Polymer blending is an efficient method for designing the performance of polymeric materials using available polymers.[1] The incorporation of dispersed elastomeric particles in a rigid matrix has attracted considerable attention because of its industrial importance of this among other types of polymer blends.[2–5] A interesting aspect of rubber toughening is required to improve interfacial adhesion, rubber particle dispersion, and stress transfer between the phases to improve the properties of the materials.[6–8]

High-impact polystyrene (HIPS) is a good example in which mechanical properties can be modified through a change in the microstructure of rubbery particles. Rubbery chains are grafted onto the rigid matrix and this grafting enhances the interfacial bonding between the phases, providing a good dispersion of the elastomeric particles in the PS matrix.[9] Besides its direct technological application, HIPS is also used in blends with other polymers, such as poly(2,6-dimethyl-1,4-phenylene oxide), which is widely applied in the automotive industry and in home appliances.[2,10–12]

Aging is a significant problem with HIPS and other rubber-toughened plastics, especially those based on polybutadiene. The major contribution to photodegradation is usually attributed to the polybutadiene phase, which is made up of different isomers that present different stabilities to degradation. Exposure to sunlight causes a drastic drop in the impact resistance as a consequence of the photooxidation of the rubber phase induced by UV radiation, which limits the lifetime in outdoor applications.[13,14] To overcome this problem, polybutadiene is replaced in blend compositions by a saturated rubber, such as poly(ethylene-*co*-vinyl acetate) (EVA), poly(butyl acrylate), or ethylene-propylene-diene terpolymer (EPDM)[15,16].

Poly(acrylonitrile-*co*-butadiene-*co*-styrene) (ABS) is another important commercial polymer that presents high impact resistance, stiffness, easy production, and processability that justify its use in the automotive industry. But ABS presents low thermal resistance and low weatherability because of the high

Correspondence to: M. I. Felisberti (misabel@iqm.unicamp.br).

level of unsaturation of its rubber phase. To overcome this problem, research in this field has led to the production of a thermoplastic with a low level of unsaturation, such as poly[acrylonitrile-*g*-(ethylene-*co*-propylene-*co*-diene)-*g*-styrene] (AES). AES is very attractive due to its appreciable impact resistance and better environmental and thermal resistance than both ABS and polybutadiene due to the low amount of unsaturation of EPDM rubber.[14] AES is a commercial elastomer obtained by radical copolymerization of styrene and acrylonitrile in the presence of EPDM. SAN [poly(styrene-*co*-acrylonitrile)] is formed, either grafted on EPDM chains or ungrafted. The final product also contains a fraction of EPDM molecules not involved in the grafting process.[17]

In an earlier article, the thermal and mechanical properties of PS/AES blends prepared by *in situ* polymerization of styrene were reported. These blends are immiscible and show complex phase behavior.[18] Furthermore, the morphology of injected specimens is quite different from that of noninjected blends. In this way, the influence of injection molding on the morphology of PS/AES is examined in the current article.

EXPERIMENTAL SECTION

Materials

Crompton Corporation (Rio Claro, Brazil) supplied AES (Royaltuf® 372P20). AES is a complex mixture of SAN, EPDM, and grafted copolymer EPDM-*g*-SAN. AES contains 13 wt % of free EPDM, 22 wt % of free SAN, and approximately 65 wt % of EPDM-*g*-SAN. The SAN presents 27 wt % of acrylonitrile content. The global composition of AES is 50 wt % of SAN and 50 wt % of EPDM. The EPDM of AES contains 68.9 wt % of ethylene, 26.5 wt % of propylene, and 4.6 wt % of 2-ethylidene-5-norbornene (ENB) as diene.[19]

Styrene monomer purification

Styrene monomer was submitted to extraction of polymerization inhibitors with a 5% NaOH solution. After this, the organic layer was washed with distilled water. The water residue was extracted with dry Na_2SO_4 and the styrene was then distilled at 50°C under vacuum.

In situ polymerization of PS/AES blends

AES was dissolved in styrene monomer under stirring, then benzoyl peroxide (0.1 wt %) was added to the viscous and homogeneous solution and the polymerization was performed at 60 or 80°C. Each polymerization reaction produced approximately 600 g of material. After this, the styrene monomer residue (~5 wt %) was extracted at 50°C in a vacuum oven for 48 h. Polystyrene homopolymer was also prepared at 60°C and 80°C. Table I shows the composition of the PS/AES blends expressed in terms of AES and EPDM contents. The AES content in the blends was calculated from the nitrogen percentage determined by elemental analysis. The nomenclature used to describe the blends is based on the EPDM content and on the temperature of polymerization. For example, the blend containing 11.5 wt % of EPDM polymerized at 60°C is named 11.5A60, where A represents the source of EPDM, i.e., AES.

TABLE I
PS/AES Blends Prepared in this Work

Name	AES (wt %)[a]	EPDM (wt %)[b]	Reaction temperature (°C)	$\overline{Mn}$ of PS ($\times 10^3$ g mol $^{-1}$)[c]	$\overline{M}_w/\overline{M}_n$[c]	$T_{g(\text{EPDM phase})}$ °C[d]	
						Before injection	After injection
3.7A60	7.3	3.7	60	271	1.7	−41	−48
4.5A60	9.0	4.5	60	265	1.7	−38	−48
6.5A60	13.0	6.5	60	283	2.1	−39	−45
7.9A60	15.8	7.9	60	268	2.3	−40	−47
9.5A60	18.9	9.5	60	298	2.3	−41	−44
11.5A60	22.9	11.5	60	316	2.1	−40	−44
7.2A80	14.4	7.2	80	98	2.3	−44	−48
8.5A80	17.0	8.5	80	188	2.9	−42	−46
9.4A80	18.8	9.4	80	187	2.1	−44	−46
10.9A80	21.8	10.9	80	173	2.2	−40	−40
PS60	—	—	60	140	2.6		
PS80	—	—	80	193	2.2		

[a] AES content obtained from elemental analysis.
[b] EPDM content obtained from AES content in the blends.
[c] GPC data for PS extracted from the blends.
[d] Glass transition temperature obtained from DSC.

Injection molding

The crushed blends were dried in a vacuum oven for 48 h at 50°C and injection molded into Izod bars (ASTM D256) and dog-bone–shaped tensile specimens (ASTMD638) using an Arburg Allrounder molding machine model 221 M 250-55 (Lossburg, Germany). The following temperatures were kept along the barrel zones: 200, 210, 220, 230, and 240°C. The mold temperature was kept at 40°C.

Extraction of polymeric phases

The components of PS/AES blends (PS, SAN, and EPDM) were continuously extracted using a Soxhlet apparatus. First, the EPDM phase was extracted with hexane, followed by extraction of the SAN phase with acetone and, finally, the linear PS chains were extracted with dichloromethane. Each extraction step was performed for 72 h. The residue left in the cellulose thimble was collected and named insoluble phase.

Fourier transformed infrared spectroscopy (FTIR)

The FTIR analyses of the films of extracted phase were performed on a FTIR Nicolet 520 spectrophotometer (Waltham, MA), using 16 scans and a resolution of 2 cm^{-1}. The films were prepared in a Marconi MA 098/A Hydraulic Press (Piracicaba, Brazil) at 150°C with 7-ton press.

Dynamic mechanical analysis (DMA)

The dynamic mechanical analysis of the noninjected and injected blends was performed in a Rheometric Scientific DMTA V Analyzer (Piscataway, NJ). The specimens (9.0 × 6.0 × 1.0 mm) were subjected to sinusoidal deformation at a frequency of 1.0 Hz and amplitude of 0.01% in the temperature range from −100 to 180°C.

Tensile and impact resistance tests

The injection-molded specimens were submitted to impact resistance and tensile tests in an EMIC AIC 1 (São José dos Pinhais, Brazil) apparatus and in an EMIC DL 200 (São José dos Pinhais, Brazil) apparatus (5000 N load cell, 5 mm min^{-1} speed), respectively.

Transmission electron microscopy

Blend morphologies were determined using a Carl Zeiss CEM902 transmission electron microscope (Thornwood, NY). The films were ultramicrotomed under cryogenic conditions (-140°C) to obtain ultrathin sections (40 nm). Phase contrast between the injected blend components was achieved by exposing the samples to vapors of OsO_4 for a period of 4 h. Micrographs of selected blends were employed for particle size analysis by a digital analysis technique based on Image Pro Plus® software. The particle size distribution as well as the weight average particle diameters, $\overline{d}w$, were determined from these results.

RESULTS AND DISCUSSION

The aim of this work was to evaluate the influence of injection molding on the dynamic mechanical and morphological behavior of PS/AES blends prepared by *in situ* polymerization of styrene. As previously reported, PS/AES blend are immiscible and present a complex phase behavior.[18]

Extraction of polymeric phases

The PS/AES blends could be understood as a quaternary mixture of PS, SAN, EPDM, and EPDM-*g*-SAN. These components present distinct solubility. The EPDM phase can be extracted with hexane, which is a nonsolvent for SAN and PS. The SAN phase can then be extracted with acetone, whereas PS phase can be extracted with dichloromethane.

Table II shows the percentage of each extracted phase (PS, SAN, EPDM, and insoluble phase) for PS/AES blends. The extraction yield is defined as the ratio between the extracted mass and the mass estimated by elemental analysis (Table I). The extraction yield of the PS phase varies from 62% (for 10.9A80) to 93% (for 3.7A60) and also as the temperature of polymerization and AES content increase. The extraction yield of SAN and EPDM is lower, between 30% for SAN phase and 20% for EPDM phase, when the latter phase is extracted. These results suggest that crosslinking as well as grafting reactions take place during the polymerization of styrene in presence of AES.

TABLE II
Percentage of Each Extracted Phase of PS/AES Blends

	Percentage of extracted phase (extraction yielding %)			
Materials	PS	SAN	EPDM	Insoluble phase
3.7A60	89.7 (93)	0.3	—	1.1
4.5A60	83.7 (88)	0.2	—	7.1
6.5A60	61.8 (66)	0.9	0.4	17.6
7.9A60	61.8 (67)	2.2	0.1	1.2
9.5A60	73.9 (82)	2.5	—	6.3
11.5A60	54.5 (62)	1.4	3.0	21.2
7.2A80	61.8 (67)	2.2	0.1	1.2
8.5A80	70.3 (78)	1.5	1.4	12.6
9.4A80	55.7 (76)	4.5	—	24.5
10.9A80	50.6 (70)	5.8	—	24.5

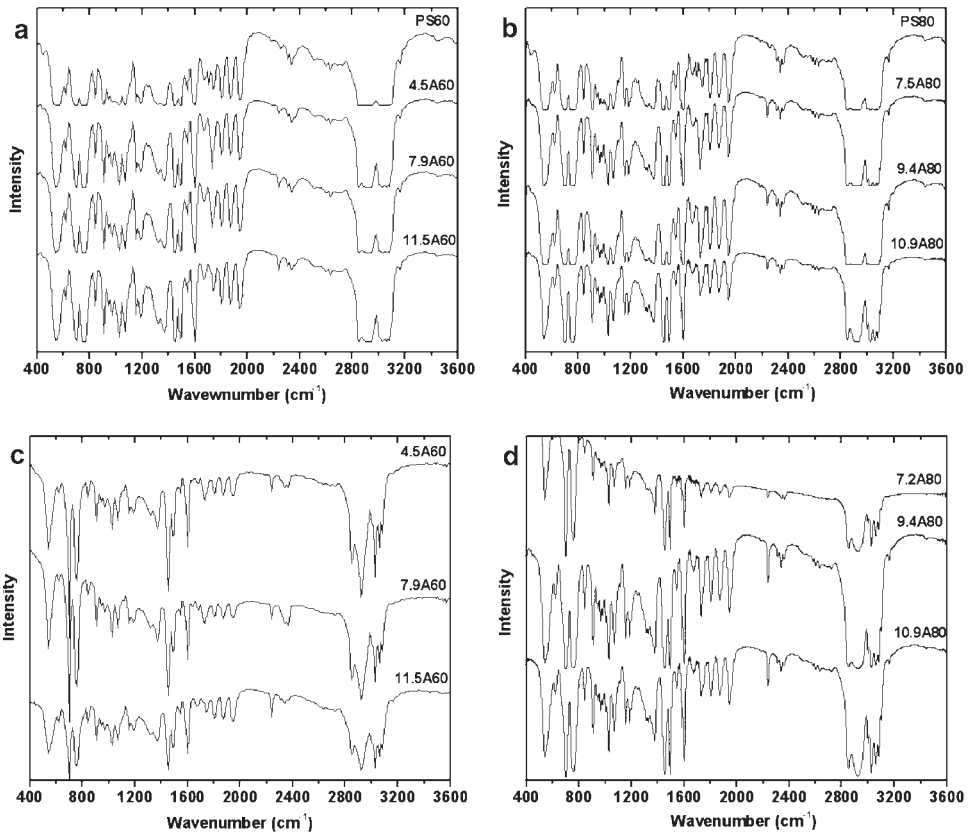

Figure 1 FTIR spectra of extracted (a,b) PS phase and (c,d) insoluble phase; blends prepared at (a,c) 60°C and (b,d) 80°C.

Figure 1(a,b) show infrared spectra of extracted PS from PS/AES blends and Figure 1(c,d) show the infrared spectra of the insoluble phase of PS/AES blends. Figure 1(a,b) show the presence of the characteristic absorption bands of the PS and also a small intense band at 2237 cm^{-1} attributed to the absorption of the nitrile group of the SAN. The following hypothesis could explain the appearance of this band: SAN phase was not completely extracted with acetone and being SAN soluble in dichloromethane, both PS and SAN were extracted in the last stage of the selective extraction (see experimental section). Figure 1(c,d) show that the insoluble phase of these blends present characteristic absorption bands of polystyrene (1600 cm^{-1} and above 3000 cm^{-1}), of acrylonitrile group of SAN (2237cm^{-1}) as well as intense bands related to absorption of the aliphatic hydrocarbon –EPDM (2950 and 2860 cm^{-1}). Thus, the insoluble phase seems to contain PS, SAN, and EPDM, probably as a complex grafted and crosslinked mixture.

Dynamic mechanical analysis (DMA)

Figure 2 shows the dynamic mechanical behavior of noninjected PS60, PS80, and PS/AES blends. The storage modulus curve of AES [Fig. 2(a)] shows a drop of one decade around −40°C corresponding to the glass transition of EPDM phase and another drop of two decades at 120°C corresponding to the glass transition of SAN phase.[14] The storage modulus curves of the noninjected PS/AES blends show a small drop in the region of EPDM glass transition (∼−40 °C) and a drop of three decades in the region of the glass transition of PS and SAN phases.

The loss modulus curves of PS60 and PS80 showed a peak around 100°C corresponding to the glass transition of PS and also a peak corresponding to the β-transition (T_β) of PS at 20°C attributed to the torsion and vibration of the phenyl group in the main chain.[20,21]

The loss modulus of AES shows a peak at −40°C corresponding to the glass transition of the EPDM phase, a peak at 120°C corresponding to the glass transition of SAN phase and a peak around 60°C corresponding to a secondary transition of the EPDM phase of AES.[21,22] The loss modulus of noninjected PS/AES blends shows a peak around −40°C corresponding to the glass transition of the EPDM phase, a peak at 20°C corresponding to the β-transition (T_β) of the PS phase and a complex phase behavior in the region of PS and SAN glass

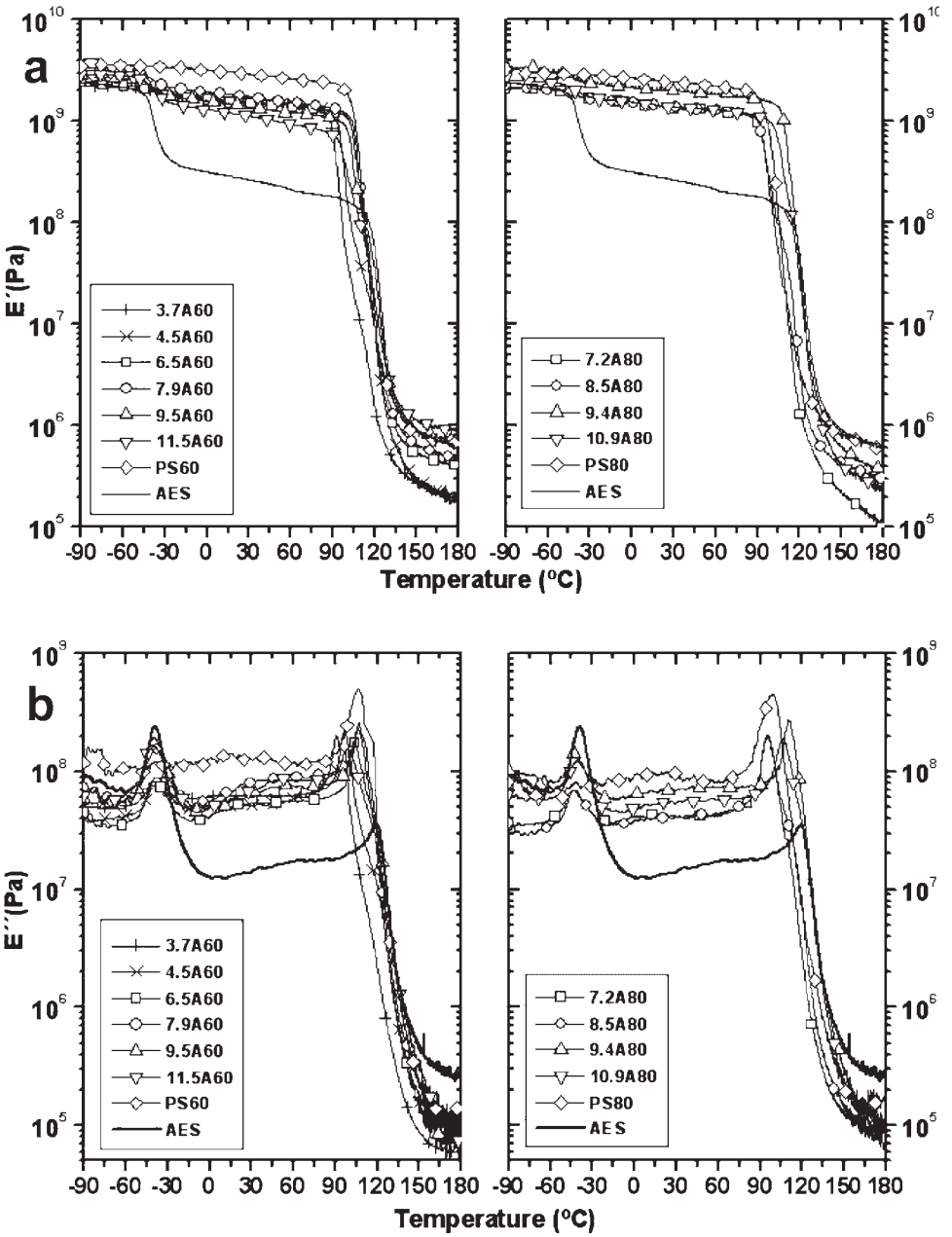

Figure 2 Dynamic mechanical behavior of noninjected PS60, PS80, AES, and PS/AES blends. (a) Storage modulus (E′) and (b) loss modulus.

transitions. The loss modulus curves in this region show a peak at lower temperatures corresponding to the glass transition of the PS phase and a shoulder at higher temperatures corresponding to the SAN phase.

Figure 3 shows the dynamic mechanical behavior of injected PS60, PS80, AES, and PS/AES blends. After injection molding, some changes in the dynamic mechanical curves of the blends can be observed. For example, the shoulder in the region of the glass transitions of PS and SAN in the storage and loss modulus curves disappears. A drop in the storage modulus and the peak in the loss modulus curves in the temperature range of the glass transition of the elastomer phase are very hard to be observed, indicating that the influence of the EPDM phase on the dynamic mechanical properties decreases. These results suggest a change in the morphology of the PS/AES blends during the injection molding process.

Besides the EPDM phase of all injection molded blends presents a glass transition temperature at lower temperatures than those of the EPDM phase of AES and EPDM phase of the noninjected blends

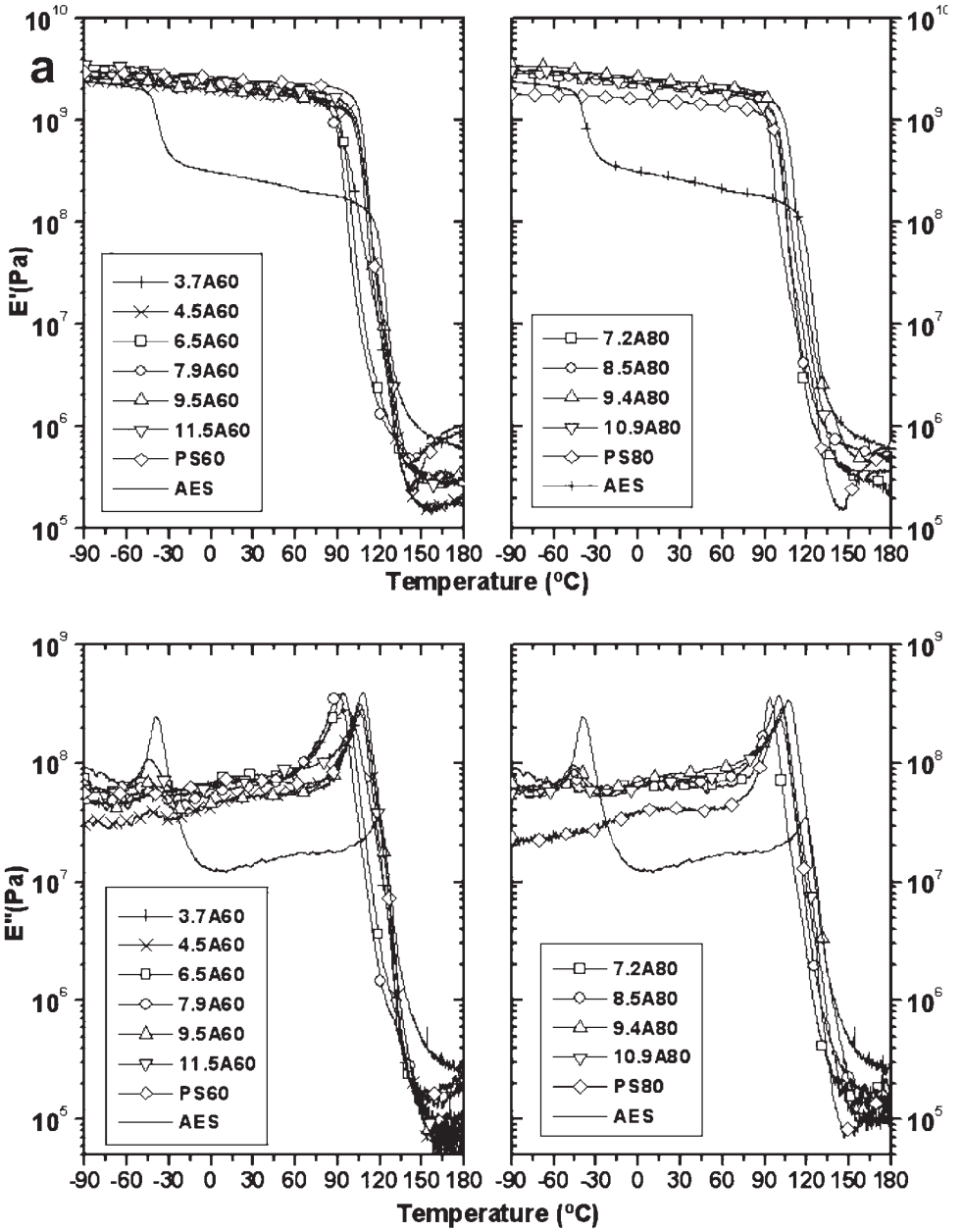

Figure 3 Dynamic mechanical behavior of injected PS60, PS80, AES and PS/AES blends. (a) Storage modulus (E′) and (b) Loss modulus (E″).

(Table I). A decrease of the glass transition temperature of the elastomer phase was also observed in earlier work of our research group for polyhydroxybutyrate/AES blends,[23] poly(methyl methacrylate)/AES blends,[24] and *in situ* polymerized PS/EPDM blends.[25] For these cases, this phenomenon was attributed to the phase inversion of the EPDM phase of AES. For PS/AES blends, the decrease of the T_g of the EPDM phase occurs after injection molding, therefore, the phase inversion occurs or completes probably during the injection molding. The decrease of the T_g of the rubbery phase is common in blends of a rubbery phase dispersed in glassy matrices and is attributed to hydrostatic dilatational thermal stresses generated within the rubber particles because of the differences in thermal expansion between the rubber and the glassy matrix.[26–29] According to Booij,[28] the smaller the elastomer content the larger is the shift of the elastomer phase transition toward lower temperatures. This dilatational stress promotes an increase in the rubbery phase free volume, which allows reduction of the relaxation time of the rubbery chains and, therefore, reduces the glass transition temperature of the corresponding phase.[14] Another condition for decreasing T_g is the good adhesion between the components.[28]

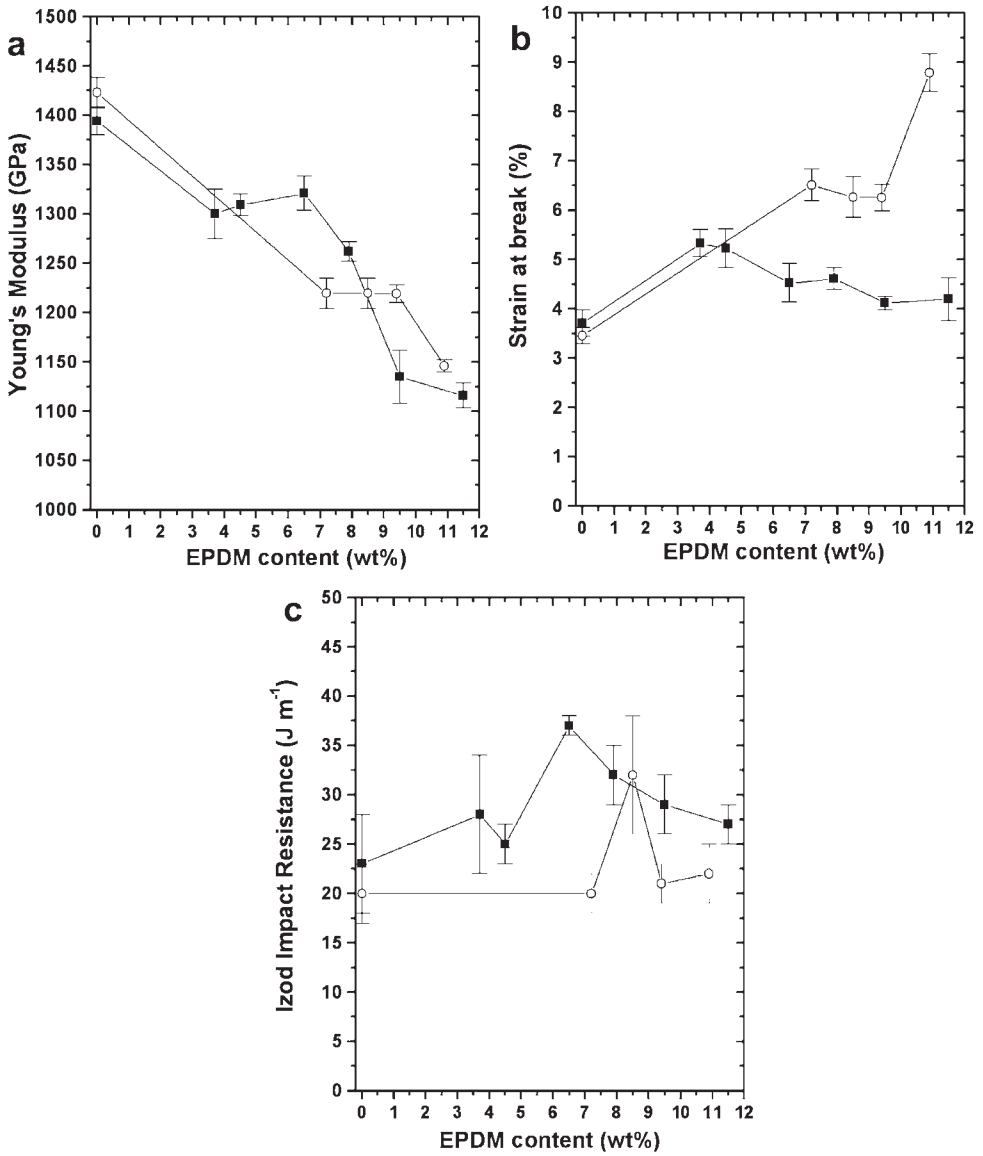

Figure 4 (a) Young's modulus, (b) strain at break, and (c) impact resistance curves as a function of EPDM content for PS/AES blends prepared at 60 (■) and 80°C (○).

Mechanical properties

Figure 4 shows the mechanical properties of the injection molding blends, such as Young's modulus, strain at break, and impact resistance. The PS/AES blends showed stress whitening during the tensile tests, indicating that dilatational processes, such as crazing and cavitation, occur during the loading.

The Young's modulus decreases 20% with the addition of 10.9 wt % of EPDM (21.8 wt % of AES) in comparison with the value of polystyrene. However, the decrease of the Young's modulus of PS/AES blends is less than the drop of Young's modulus of *in situ* polymerized PS/EPDM blends with comparable contents of elastomer, due to the stiffening of PS promoted by the SAN phase.[25]

In general, PS/AES blends polymerized at 80°C present higher strain at break than blends obtained at 60°C. The PS/AES blend prepared at 80°C containing 10.99 wt % of EPDM (21.8 wt % of AES) presents higher strain at break, 8.8%, against 4.5% for the blend with similar composition obtained at 60°C.

The impact resistances are higher for blends prepared at 60°C than for those prepared at 80°C. For the blends prepared at 60°C, an increase of the EPDM content up to 6.55 wt % (13.0 wt % of AES) led to an increase of 60% in the impact resistance and further increases in the AES content led to a slight decrease in impact resistance. For the blends prepared at 80°C, the impact resistance is practically constant and equal to the value of PS80, except for

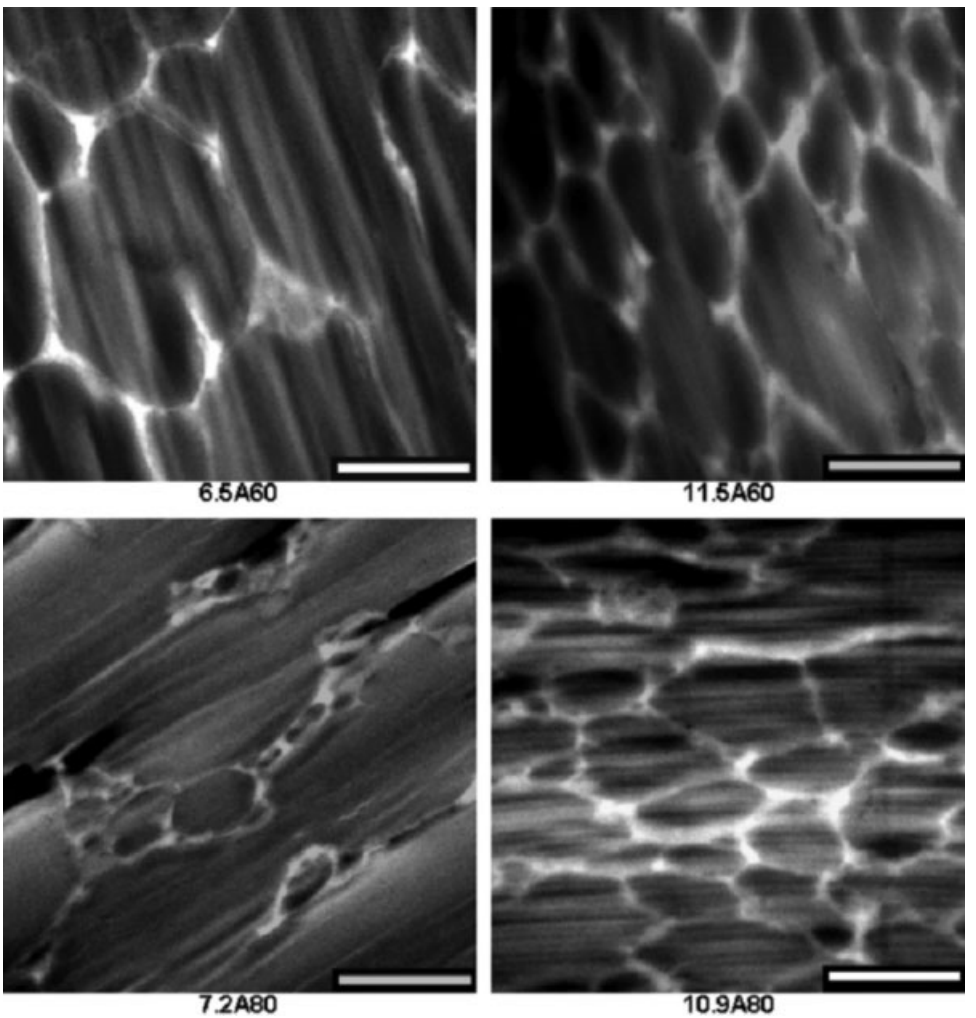

Figure 5 TEM micrographs of noninjected PS/AES blends. Scale bars correspond to 1 μm.

the blend containing 8.55 wt % of EPDM (17.0 wt % of AES).

Transmission electron microscopy

Figure 5 shows the TEM micrographs of noninjected PS/AES blends. The analyzed cuts were not stained because the phase contrast was good enough to identify the different phases: polystyrene is the dark phase. Figure 6 shows the TEM micrographs of injection-molded PS/AES blends. In this case, the thin sections were stained to improve the contrast between the phases and the rubber particles became the dark phase. There is a great difference between the morphologies of noninjected and injected blends. The morphology of noninjected blends consists of spherical domains of PS surrounded by the AES phase, whereas the morphology of injected blends is an elastomeric dispersed phase. Three factors could contribute to this drastic change of morphology: (1) the stationary polymerization conditions did not allow the mixture to reach the equilibrium morphology; (2) the grafting degree between PS and AES was not high enough to ensure the morphological stability against changes during processing in the melting state; and (3) the viscosity of elastomer phase is much greater than that of resin during injection. Much large viscosity and small composition of elastomer make it dispersed during deformation.

The change of the morphology explains some differences in the dynamic mechanical behavior of the blends before and after injection molding, such as those observed in the temperature range of EPDM glass transition. However, this drastic morphological change did not alter significantly the mechanical properties of the blends, as observed, for example, for PS/EPDM blends prepared by *in situ* polymerization before and after injection molding,[30] for those, the dynamic mechanical properties as well as the morphology differ considerably. EPDM and AES blends differ by the presence of SAN (50 wt %). As

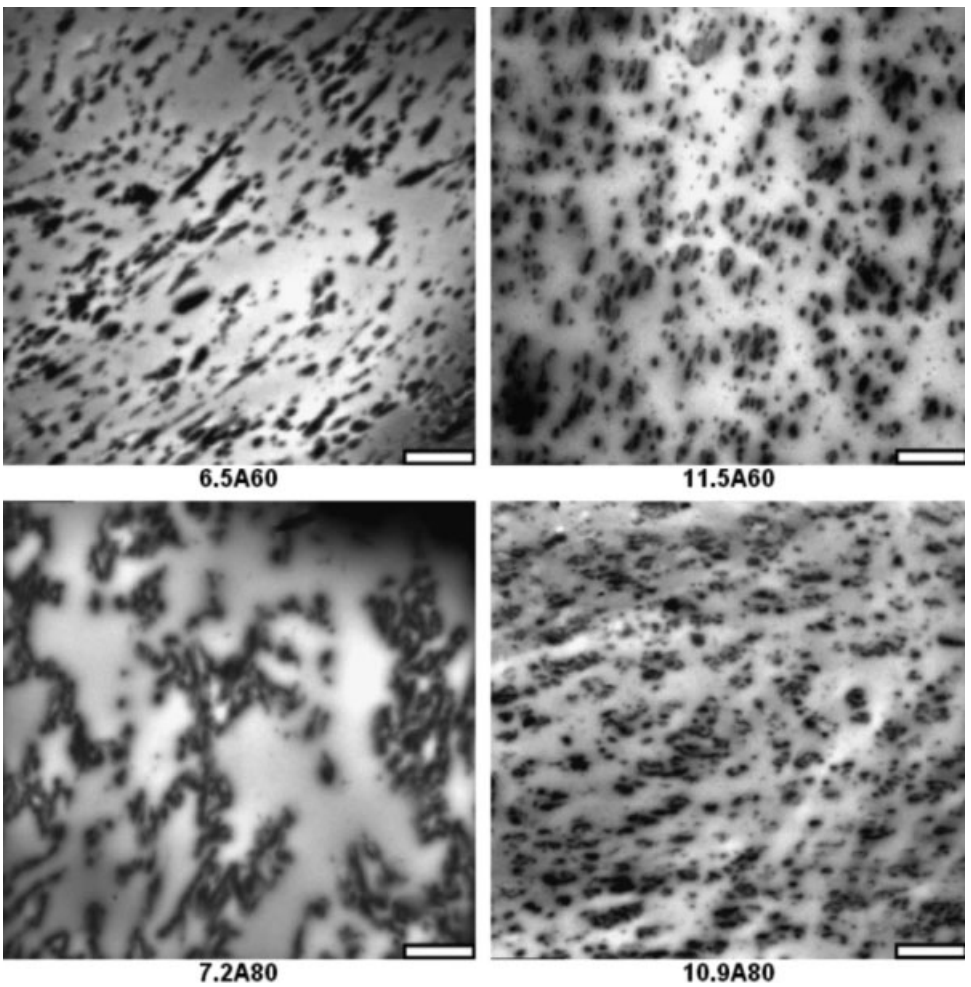

Figure 6 TEM micrographs of injected PS/AES blends. Rubber particles are stained dark by OsO_4. Scale bars correspond to 1 μm.

discussed above, the continuous phase of the noninjected blends is AES and the maximal concentration of this elastomer in the blends is 21.8 wt % (10.9 wt % of EPDM). Thus, the presence of a rigid SAN copolymer phase seems to be responsible for keeping the storage modulus in the temperatures between the glass transition of EPDM and PS/SAN phases.

The morphology of the blends before and after injection molding presented important differences in comparison to the salami morphology of HIPS. The main difference is the absence of PS microoclusions in the EPDM domains, which promote a higher tensile stress for the elastomeric phase. Moreover, the diameter of the elastomeric domains of the blends of this work is smaller than the critical size for PS toughening described in literature.[31]

Figure 7 shows the histograms for the quantitative analysis of the diameter of the EPDM particles. The average diameter of rubber particles of each composition was calculated by image analysis. The results in Table III show that the average diameter of PS/AES blends does not change significantly as the elastomer content and polymerization temperature increase.

A minimum effective particle diameter of 0.040 μm for the toughening of PS was established, because the stress-concentration zone must not be smaller than the minimum craze thickness.[32,33] However, it is accepted that small particles (<1 μm) reinforce PS to a much lesser degree than do large particles (2–5 μm) at constant rubber content.[33] Particles whose diameters are significantly greater than an optimum domain size (2–5 μm) are less effective for craze initiation. The elastomer domains in the PS/AES blends present the average diameter lower than 80 nm (see Table III). Thus, the improvement of the mechanical properties of PS by polymerization of styrene in presence of AES should not be expected. Despite this, a small enhance of the strain at break is observed for blends prepared at 80°C [see Figure 4(b)].

Comparing the average diameters (Table III) of PS/AES and PS/EPDM,[30] both obtained by *in situ* polymerization, it can be seen that the average

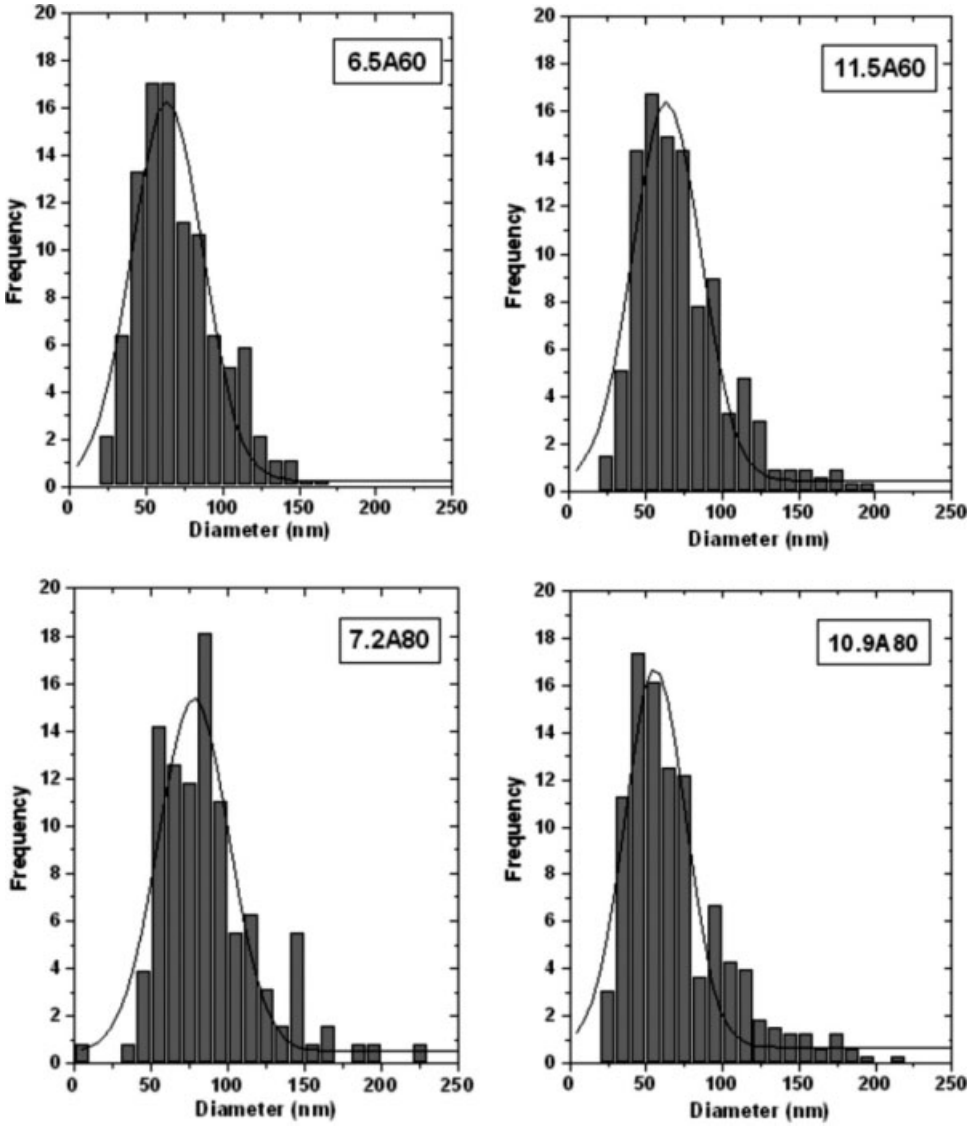

Figure 7 Rubber particle size distribution obtained from TEM micrographs of selected PS/EPDM blends.

diameter is smaller for the PS/AES blends. However, the strain at break of the blends PS/EPDM is higher in comparison with blends PS/AES. The first observation is possibly due to the presence of SAN in the AES elastomer that decreases the interfacial tension. The second observation can be understood as a domain size effect as discussed above. Thus, the mechanical properties of PS/AES are a compromise between interfacial adhesion and domain size. Similar behavior was reported for blends of PS and polyurethane rubber.[34,35]

TABLE III
Weight Average Diameter of Rubber Particles Calculated from TEM Micrographs

	Material	Weight average diameter (nm)
PS/AES	6.5A60	64 ± 2
	11.5A60	78 ± 2
	7.2A80	64 ± 2
	10.9A80	56 ± 2
PS/EPDM	5E60	102 ± 2
	17E60	130 ± 2
	5E80	189 ± 9
	17E80	231 ± 6

CONCLUSION

The morphology of the injected blends is quite different from that of the noninjected blends. The TEM micrographs showed that the morphology of noninjected PS/AES blends consists of PS spherical domains surrounded by the EPDM phase, whereas the morphology of injected blends shows an elastomeric dispersed phase. The average diameter as well as the diameter distribution is smaller for the PS/AES blends than for the PS/EPDM blends,[33] suggesting that the SAN phase of the AES acts as compatibilizer

between PS and EPDM phases and promoting a better dispersion of the elastomeric phase.

Acknowledgment

The authors thank FAPESP (Proc.: 03/04246-2) for financial support.

References

1. Galloway, J. A.; Jeon, H. K.; Bell, J. R.; Macosko, W. Polymer 2005, 46, 183.
2. Ohishi, H.; Ikehara, T.; Nishi, T. J Appl Polym Sci 2001, 80, 2347.
3. Katime, I.; Quintana, J. R.; Price, C. Mater Lett 1995, 22, 297.
4. Ramsteiner, F.; Heckmann, W.; MacKee, G. E.; Breulmann, M. Polymer 2002, 42, 5995.
5. Socrate, S.; Boyce, M. C.; Lazzeri, A. Mech Mater 2001, 33, 155.
6. Bucknall, C. B. In Comprehensive Polymer Science; Allen, G.; Bevington, J. C.; Eastmond, G. C.; Ledwith, A.; Russo, S.; Sigwalt, P., Eds.; Pergamon Press: Oxford, 1989; Vol. 10, pp 27–47.
7. Wu, J.; Guo, B.; Chan, C.-H.; Li, J.; Tang, H.-S. Polymer 2001, 42, 8857.
8. Dompas, D.; Groeninckx, G. Polymer 1994, 35, 4743.
9. Choi, J. H.; Ahn, K. H.; Kim, S. Y. Polymer 2000, 41, 5229.
10. Amado, F. D. R.; Gondran, E.; Ferreira, J. Z.; Rodrigues, M. A. S.; Ferreira, C. A. J Membr Sci 2004, 234, 139.
11. Alfarraj, A.; Nauman, E. B. Polymer 2004, 45, 8435.
12. Matisová-Rychlá, L.; Ryhlý, J.; George, G. A. Polym Degrad Stab 2002, 75, 385.
13. Saron, C.; Felisberti, M. I. Mater Sci Eng A 2004, 370, 293.
14. Larocca, N. M.; Hage, E., Jr; Pessan, L. A. Polymer 2004, 45, 5265.
15. Tanabe, T.; Furukawa, H.; Okada, M. Polymer 2003, 44, 4765.
16. Hwang, I. J.; Lee, M. H.; Kim, B. K. Eur Polym J 1998, 34, 671.
17. Turchet, R.. Blendas de PMMA e AES: Morfologia e Propriedades Mecânicas, Master's Thesis, Instituto de Química, Universidade Estadual de Campinas, 2002.
18. Lourenço, E.; Felisberti, M. I. J Appl Polym Sci 2007, 105, 986.
19. Turchette, R.; Felisberti, M. I. Polímeros:Ciência e Tecnologia 2006, 16, 158.
20. Ko, J.; Park, Y.; Choe, S. J Polym Sci: Polym Phys 1998, 36, 1981.
21. Sheng, J.; Li, F.-K.; Hu, J. J Appl Polym Sci 1998, 67, 1199.
22. Keinath, S. E.; Boyer, R. F. J Appl Polym Sci 1981, 26, 2077.
23. Carvalho, F. P.; Quental, A. C.; Felisberti, M. I. J Appl Polym Sci 2008, 110, 880.
24. Turchet, R.; Felisberti, M. I. J Appl Polym Sci, submitted.
25. Lourenço, E.; Felisberti, M. I. Eur Polym J 2006, 42, 2632.
26. Szabó, P.; Epacher, E.; Földes, E.; Pukánsky, E. Mater Sci Eng A 2004, 383, 307.
27. Bucknal, C. B. J Microscopy 2001, 201, 221.
28. Booij, H. C. Br Polym J 1977, 9, 47.
29. Mäder, D.; Bruch, M.; Maier, R.; Stricker, F.; Mülthaupt, R. Macromolecules 1999, 32, 1252.
30. Lourenço, E. "Caracterização de Poliestireno de Alto Impacto à base de elastômeros saturados de EPDM", PhD Thesis, Instituto de Química, Universidade Estadual de Campinas, Campinas, Brazil, 2007.
31. Paul, D. R.; Bucknall, C. B.Polymer Blends; John Wiley & Sons, Inc.: New York, 1999.
32. Piorkowska, E.; Argon, A. S.; Cohen, R. E.; Schneider, M.; Pith, T.; Lambla, M. Polymer 1993, 34, 4435.
33. Schneider, M.; Pith, T.; Lambla, M. J mater Sci 1997, 32, 5191.
34. Cassu, S. N.; Felisberti, M. I. J Appl Polym Sci 2002, 83, 830.
35. Cassu, S. N.; Felisberti, M. I. J Appl Polym Sci 2004, 93, 2297.